ISSN: 2456-219X

Journal Of Mechanical Engineering And Biomechanics Volume 11 Issue 1 April 2026

COMPUTATIONAL FLUID DYNAMICS ANALYSIS AERODYNAMIC LIFT AND DRAG ON A VEHICLE

Dr. P. Vinod Kumar Naidu[1]
V. Jyothsna Praveen[2], B. Manikanta[3], K. Vivek Kumar[4], A. Rakesh Babu[5]

[1]Assistant Professor, Department of Mechanical Engineering
Pragati Engineering College (Autonomous)
(Affiliation to JNTUK)
Surampalem,Kakinada-533437

[2,3,4,5]Students, Department of Mechanical Engineering
Pragati Engineering College (Autonomous)
(Affiliation to JNTUK)
Surampalem,Kakinada-533437
Mail.Id: vinodnaidu12@gmail.com[1], Mail.Id: jyothsnapraveen49@gmail.com[2]
Mail.Id: bmanikanta035@gmail.com[3], Mail.Id: vivekkumarkotte@gmail.com[4]
Mail.Id: 270504rakesh@gmail.com[5]

Abstract

Aerodynamic drag and lift play a critical role in determining the fuel efficiency, stability, and overall performance of road vehicles. With increasing fuel consumption and stricter emission norms, the reduction of aerodynamic drag has become a key objective in vehicle design. This study presents a computational fluid dynamics (CFD) analysis of external flow over a road vehicle to evaluate aerodynamic drag and lift characteristics. The investigation focuses on the influence of vehicle geometry, flow separation, wake formation, engine cooling drag, wheel rotation, and crosswind effects. A three-dimensional steady-state Reynolds-Averaged Navier–Stokes (RANS) approach is adopted using suitable turbulence models. The numerical results provide insight into pressure distribution, velocity vectors, wake structure, and aerodynamic coefficients. The study demonstrates that streamlined rear-end geometry significantly reduces pressure drag and improves aerodynamic performance. The findings highlight the effectiveness of CFD as a complementary tool to wind tunnel testing in automotive aerodynamic design.

Keywords: Aerodynamics, Computational Fluid Dynamics, Drag Coefficient, Lift, Vehicle Aerodynamics, Wake Flow

1. Introduction

Aerodynamic drag is one of the most significant factors affecting vehicle fuel efficiency, particularly at speeds above 70 km/h. Along with engine efficiency and vehicle weight, aerodynamic drag governs the energy consumption of road vehicles. Even a small reduction in the drag coefficient can result in a noticeable improvement in fuel economy. With the rapid growth in the number of vehicles worldwide, reducing aerodynamic losses has become essential for conserving energy and reducing emissions.

Road vehicles behave as bluff bodies, and the flow around them is complex due to partial attachment and separation. Flow separation at the rear end creates a low-pressure wake region, leading to increased pressure drag. Additionally, unsteady wind conditions, crosswinds, engine cooling airflow, and wheel rotation further influence aerodynamic forces and moments acting on a vehicle.

EFFECT:

Aerodynamic drag (Wind resistance) which is directly proportional to the square of the speed and is also a function of shape, becomes a major factor influencing the fuel economy at speeds beyond 70 Km /Hr .The drag, lift, the crosswind force act simultaneously on the vehicle when it is in the motion & these forces cause pitching moment, rolling moment & yawing moment.

$$F = f(\rho, V, D, \upsilon, \kappa)$$

i.e $F = f(\rho, V^2, D^2, \frac{V*D}{\upsilon}, M)$

i.e. $F = f(\rho, V^2, D^2, R_e, M)$

$$R_e = \frac{\rho * V * L}{\mu} = \frac{V * L}{\upsilon}$$

, **Strouhal number** , $S_r = \frac{f * L}{V}$

Peclet number $P_e = \frac{L * V}{D} = R_e * S_c$

Schmidt number given by $S_c = \frac{\upsilon}{D} = \frac{\mu}{\rho * D}$

Fig1 Zonal approach for flowfield around the car

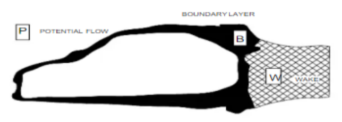

P -Potential Flow , B- Boundary Layer , W- Wake

2. Literature Review

Extensive research has been conducted on the aerodynamics of road vehicles using experimental and numerical techniques. Previous studies have shown that pressure drag contributes nearly 80–85% of the total aerodynamic drag in bluff-body vehicles, while viscous drag accounts for the remaining portion. The rear-end geometry, particularly the base slant angle, plays a dominant role in wake formation and pressure recovery.

1 Source

The literature for the topic is found from SAE transactions, Science direct, Elsevier journal & e-books on the topic of Aerodynamics, Computational fluid dynamics, Turbulence modelling, Fluid dynamics, Numerical methods & Measurements.

DOE Statistics

ISSN: 2456-219X
Journal Of Mechanical Engineering And Biomechanics Volume 11 Issue 1 April 2026

It is worth noting from the statistics given by DOE, that 16 % of the energy consumed in USA is consumed in overcoming drag of road vehicles.

Drag Reduction Technologies

It is shown that the majority of the energy consumed by ground transportation issued to overcome pressure drag rather than skin friction (Viscous) drag.

Generic Shapes

There are three generic shapes in all namely Square back, Fastback & Notchback (Three box version) depending upon the base / rear slant angle. Experimental Investigations Thomas More investigated experimentally using wind tunnels the effect of base slant (rear-end surface over which the flow is separated) on the drag generated.

Vehicle like bluff body (Morel body) 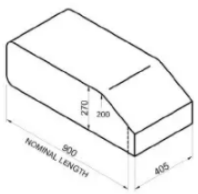	Larger wind tunnel - sca automobiles ,L/B/H vehicle bo 1(Roughly ¼ th size of a Reynold's Number $1.4*10^6$, 58 m/s, Interchangeable afte angles from 0^0 to 90^0 .Total 19 10^0 in the regions of lesser im & 2.5^0 in the regions of rapid c angle 30^0 , Drag max/min 0.41.

In general the Square back (No slant in the rear)

Design suffers from a large recirculation region behind the body due to flow separation, which results in higher drag coefficients owing to lower base pressures at the rear.

In case of Fast back (Boat tail ramp in the rear)

Designs the flow is complex due to interaction of the longitudinal vortices and separation in the rear. The Notchback

Design of car bodies refers to the three box version which has a boat tail ramp to accommodate streamlines behind the body and minimal shedding of vortices and thus avoid separation.

ENGINE COOLING DRAG

Engine cooling drag is defined as the increase in vehicle drag from a closed frontend reference condition.

$$\frac{\Delta D_{cooling}}{q_0 A_r} = 2C_{tinlet}\left(1+x_m\right)\left(\frac{V_r}{V_0}\right)+\left(-2C_{texit}\frac{A_r}{A_0}\cos\alpha\right)\left(\frac{V_r}{V_0}\right)^2$$

CROSS WINDS we know that road vehicles operate entirely in the unsteady transient conditions created by the natural wind and the wakes of other vehicles
WIND TUNNEL ISSUES:

The conventional method of testing aerodynamic properties of the vehicle has been "wind tunnel testing."

THE SYNERGY

The research work done mainly consists of CAD modelling from the image of the car with Pro-e & CFD simulation of these models using Fluent software.

JMEB
Journal Of Mechanical Engineering And Biomechanics
ISSN: 2456-219X
Volume 11 Issue 1 April 2026

3. Aerodynamic Forces Acting on a Vehicle

The primary aerodynamic forces acting on a moving vehicle are drag, lift, and side force. These forces also generate moments such as pitching, rolling, and yawing moments, which influence vehicle stability.

The aerodynamic force can be expressed as:

F=12ρV2ACF = \frac{1}{2} \rho V^2 A CF=21ρV2AC

where
ρ = air density,
V = vehicle velocity,
A = reference area,
C = aerodynamic coefficient (drag or lift).

At typical road vehicle speeds, the flow is incompressible (Mach number < 0.3). The Reynolds number is high, resulting in predominantly turbulent flow. Due to the complex nature of flow separation and wake formation, the vehicle aerodynamic analysis requires careful consideration of boundary layers and turbulence modelling.

4.3 Governing Equations

The flow is assumed to be steady, incompressible, and turbulent. The Reynolds-Averaged Navier–Stokes (RANS) equations are solved along with appropriate turbulence models. The SST k–ω turbulence model is employed due to its ability to predict flow separation under adverse pressure gradient as functional minimization.

4.Numerical Methodology

4.1 Vehicle Geometry and Domain

A simplified vehicle geometry representing a generic car shape is used for the CFD analysis. The computational domain is designed to minimize blockage effects and ensure accurate flow development upstream and downstream of the vehicle.

4.2 Mesh Generation

A three-dimensional unstructured mesh is generated with refined grid regions near the vehicle surface and wake zone to capture boundary layer effects and flow separation accurately. Mesh independence is ensured by refining the grid until variations in drag and lift coefficients become negligible.

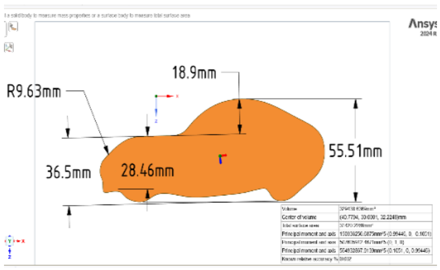

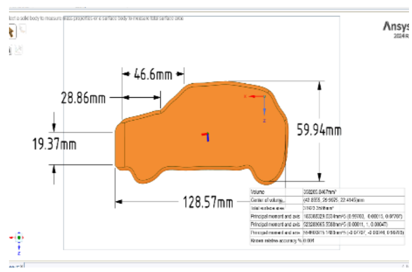

ISSN: 2456-219X
Journal Of Mechanical Engineering And Biomechanics
Volume 11 Issue 1 April 2026

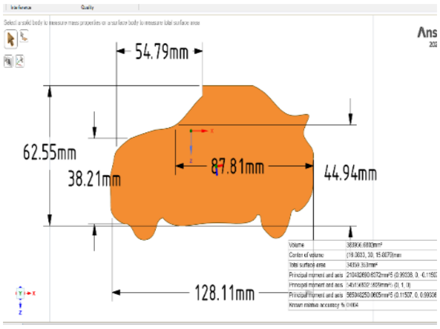

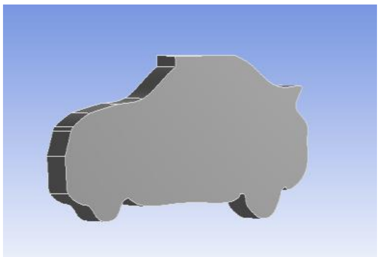

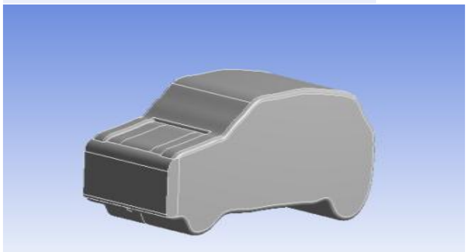

Computational fluid dynamics (CFD) is a branch of fluid mechanics that uses numerical analysis and data structures to analyze and solve problems that involve fluid flows.However, if the environment is too hostile for such delicate laboratory equipment or if it is simply not available, static pressure and temperature measurements complemented by pitot-static tube traverses can also be useful to validate some aspects of a flow field.

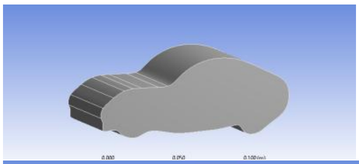

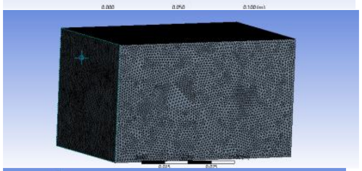

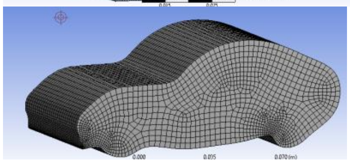

COMPUTATIONAL

FLUID DYNAMICS:

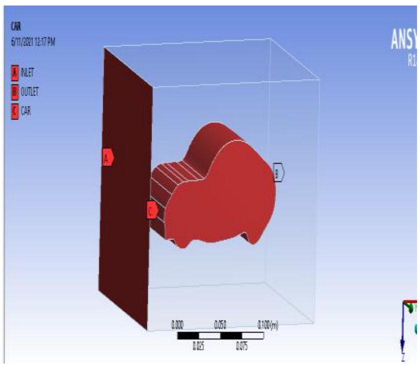

4.4 Boundary Conditions

- Inlet: Uniform velocity corresponding to road vehicle speed

ISSN: 2456-219X
Journal Of Mechanical Engineering And Biomechanics Volume 11 Issue 1 April 2026

- Outlet: Pressure outlet with atmospheric pressure
- Vehicle surface: No-slip wall condition
- Domain walls: Symmetry or slip conditions

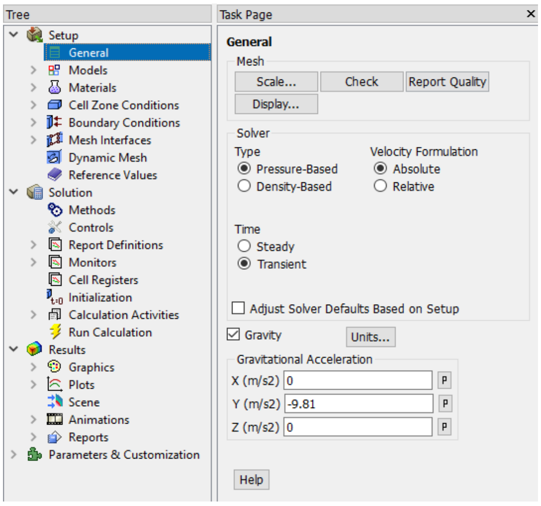

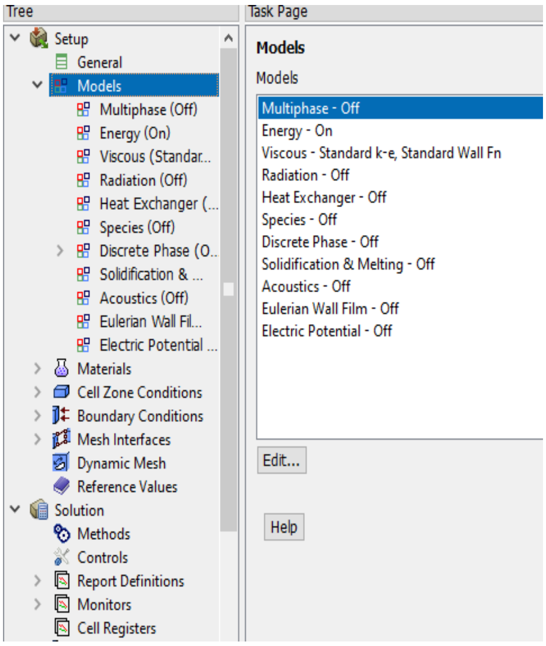

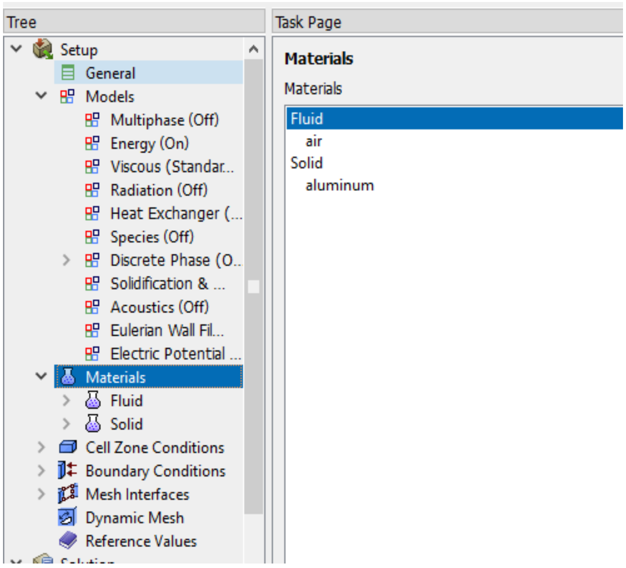

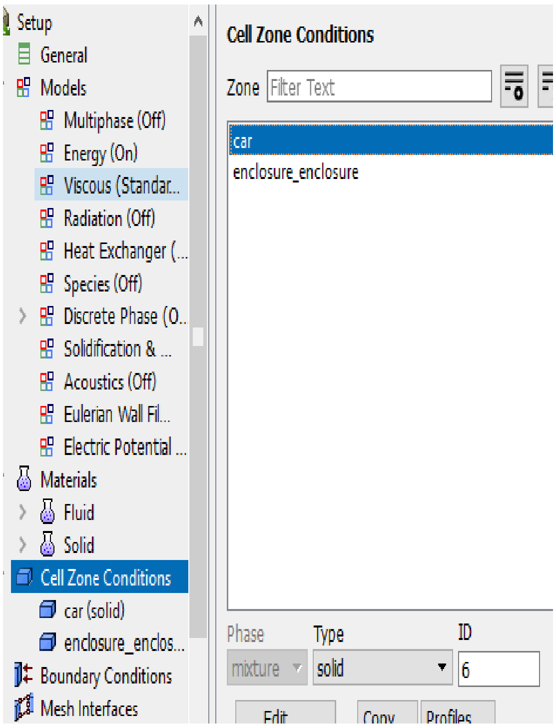

ISSN: 2456-219X
Journal Of Mechanical Engineering And Biomechanics
Volume 11 Issue 1 April 2026

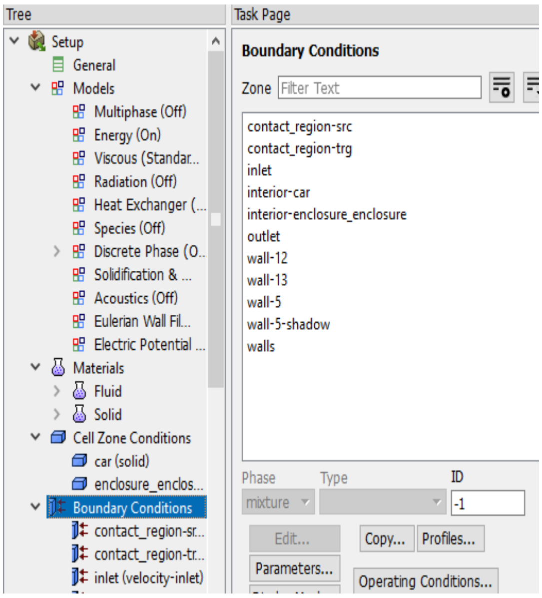

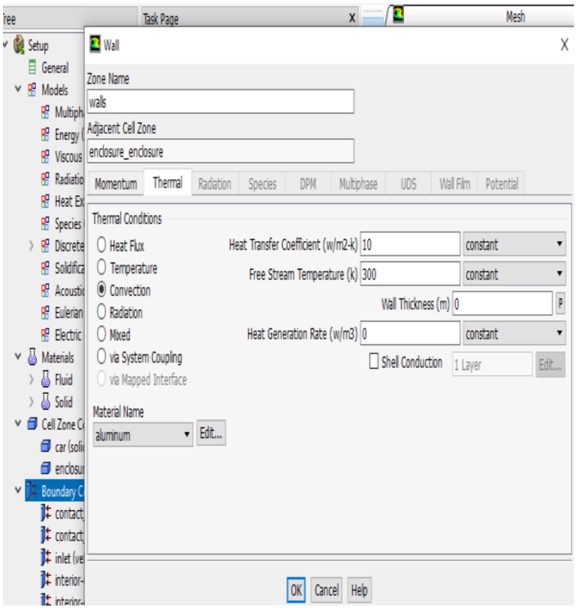

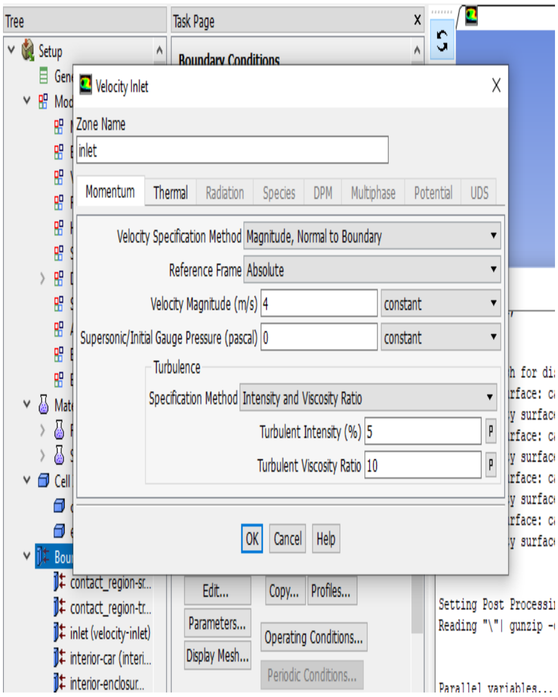

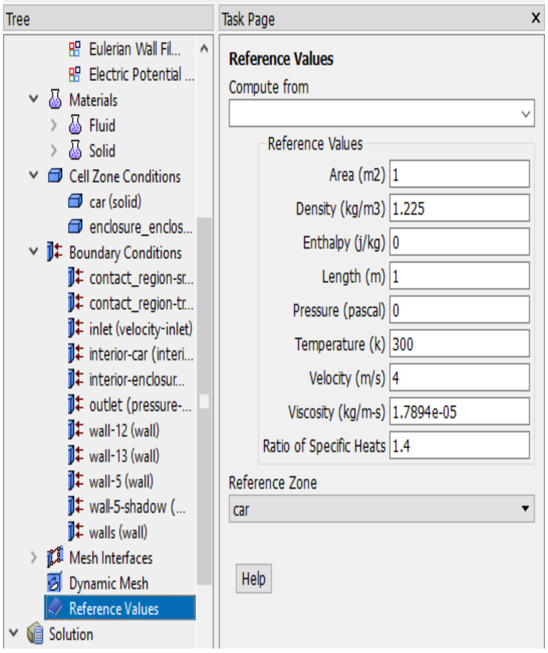

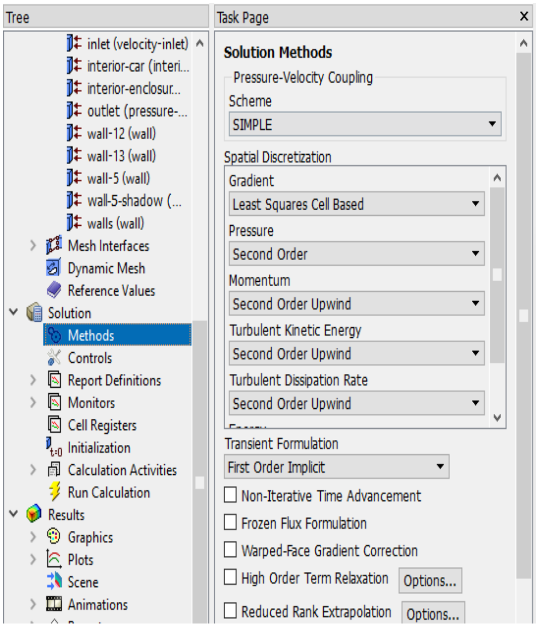
Tree
Task Page
Solution Methods
Pressure-Velocity Coupling
Scheme
SIMPLE
Spatial Discretization
Gradient
Least Squares Cell Based
Pressure
Second Order
Momentum
Second Order Upwind
Turbulent Kinetic Energy
Second Order Upwind
Turbulent Dissipation Rate
Second Order Upwind
Transient Formulation
First Order Implicit
Non-Iterative Time Advancement
Frozen Flux Formulation
Warped-Face Gradient Correction
High Order Term Relaxation
Reduced Rank Extrapolation
Options...
inlet (velocity-inlet)
wall-12 (wall)
wall-13 (wall)
wall-5 (wall)
walls (wall)
Mesh Interfaces
Dynamic Mesh
Reference Values
Solution
Methods
Controls
Report Definitions
Monitors
Cell Registers
Initialization
Calculation Activities
Run Calculation
Results
Graphics
Plots
Scene
Animations

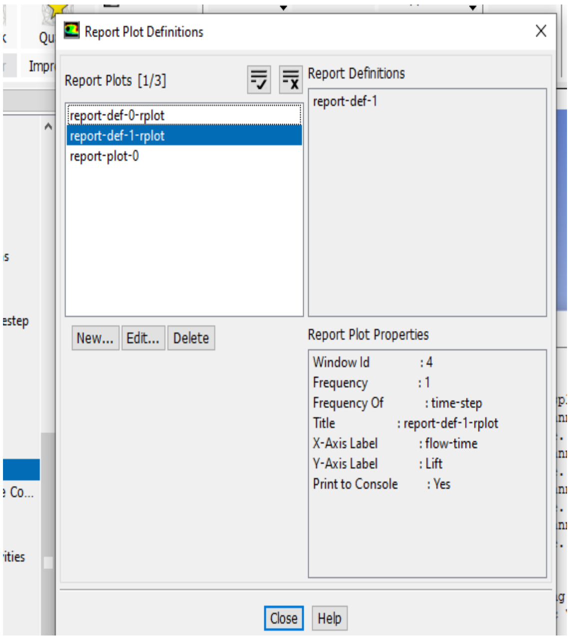
Report Plot Definitions
Report Plots [1/3]
Report Definitions
report-def-0-rplot
report-def-1-rplot
report-plot-0
report-def-1
New...
Edit...
Delete
Report Plot Properties
Window Id : 4
Frequency : 1
Frequency Of : time-step
Title : report-def-1-rplot
X-Axis Label : flow-time
Y-Axis Label : Lift
Print to Console : Yes
Close
Help

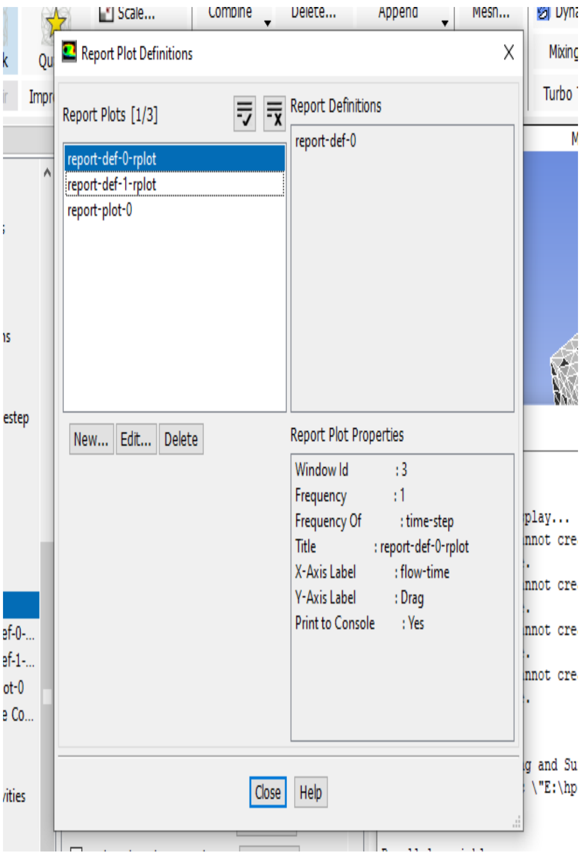
Report Plot Definitions
Report Plots [1/3]
Report Definitions
report-def-0-rplot
report-def-1-rplot
report-plot-0
report-def-0
New...
Edit...
Delete
Report Plot Properties
Window Id : 3
Frequency : 1
Frequency Of : time-step
Title : report-def-0-rplot
X-Axis Label : flow-time
Y-Axis Label : Drag
Print to Console : Yes
Close
Help

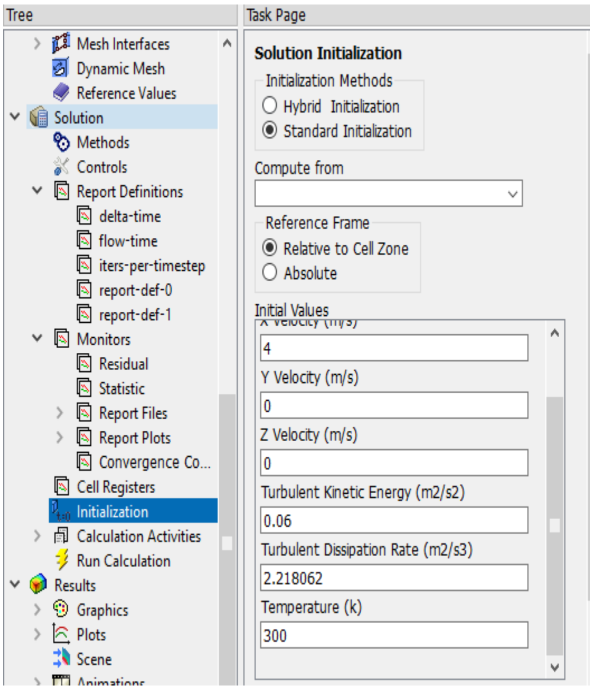
Tree
Task Page
Mesh Interfaces
Dynamic Mesh
Reference Values
Solution
Methods
Controls
Report Definitions
delta-time
flow-time
iters-per-timestep
report-def-0
report-def-1
Monitors
Residual
Statistic
Report Files
Report Plots
Cell Registers
Initialization
Calculation Activities
Run Calculation
Results
Graphics
Plots
Scene
Solution Initialization
Initialization Methods
Hybrid Initialization
Standard Initialization
Compute from
Reference Frame
Relative to Cell Zone
Absolute
Initial Values
4
Y Velocity (m/s)
0
Z Velocity (m/s)
0
Turbulent Kinetic Energy (m2/s2)
0.06
Turbulent Dissipation Rate (m2/s3)
2.218062
Temperature (k)
300

ISSN: 2456-219X
Journal Of Mechanical Engineering And Biomechanics
Volume 11 Issue 1 April 2026

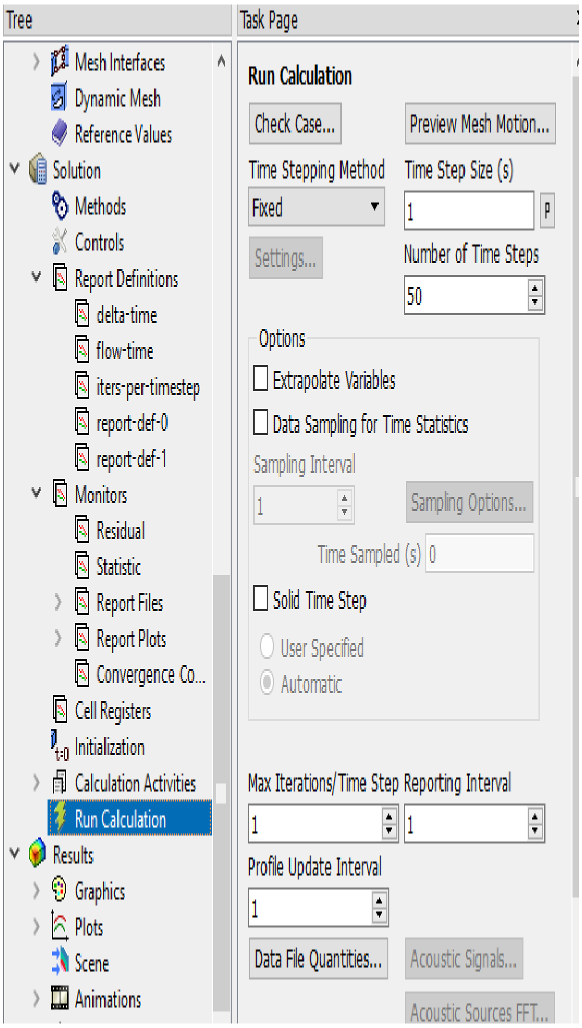

5.Resultsand Discussion

5.1 Pressure Distribution

The pressure contours reveal high-pressure regions at the vehicle front stagnation point and low-pressure zones along the roof and rear end. The rear wake region exhibits significantly reduced pressure, which contributes to pressure drag.

5.2 Velocity Field and Wake Structure

Velocity vectors show accelerated flow over the roof and strong recirculation in the wake region behind the vehicle. The size and intensity of the wake depend on the rear-end geometry. Streamlined shapes reduce wake size and improve pressure recovery.

5.3 Drag and Lift Characteristics

The computed drag coefficient values indicate that vehicles with elliptical or notchback rear profiles experience lower drag compared to flat or square-back designs. Lift coefficients are influenced by underbody flow and wheel rotation, with improper flow control leading to undesirable lift forces.

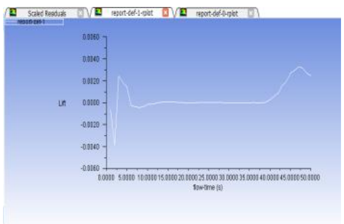

5.4 Effect of Wheel Rotation

Simulations incorporating wheel rotation show a reduction in drag due to altered wake interaction, particularly at the rear wheels. The results emphasize the importance of including wheel rotation in realistic vehicle aerodynamic simulations.

ISSN: 2456-219X
Journal Of Mechanical Engineering And Biomechanics Volume 11 Issue 1 April 2026

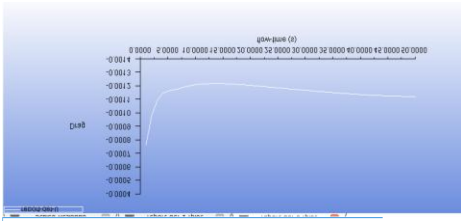

Net (0.066951868 0.018028971 0.030552659) (0.014319936 -5.8672106e-05 -6.0823784e-05

Forces - Direction Vector (1 0 0)

	Forces (n)			Coefficients		
Zone	Pressure	Viscous	Total	Pressure	Viscous	Total
wall-5-shadow	0.066951868	0.0033401214	0.070291989	0.0068318232	0.00034082871	0.007172
wall-5	0	0	0	0	0	0
wall-13	-3.5669236e-18	1.3635209e-07	1.3635209e-07	-3.639718e-19	1.3913478e-08	1.391347
wall-12	0	0	0	0	0	0
walls	0	0.010979678	0.010979678	0	0.0011203753	0.001120
Net	0.066951868	0.014319936	0.081271804	0.0068318232	0.001461218	0.008293

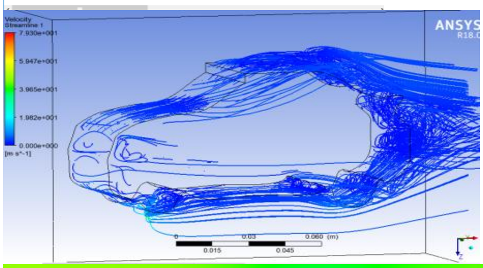

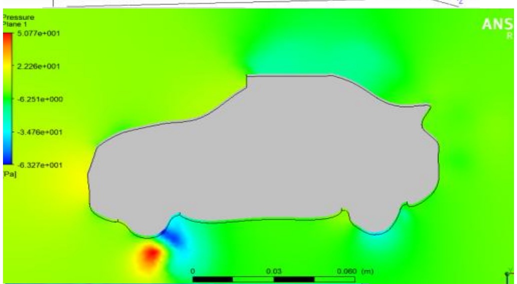

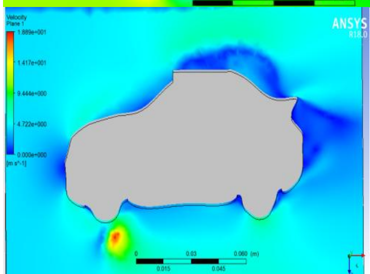

Forces - Direction Vector (1 0 0)

	Forces (n)			Coefficients		
Zone	Pressure	Viscous	Total	Pressure	Viscous	Total
wall-5-shadow	0.052027349	0.0039304412	0.05595779	0.0053089132	0.00040106543	0.005709
wall-5	0	0	0	0	0	0
wall-13	-8.5665515e-18	1.6697449e-07	1.6697449e-07	-8.7413791e-19	1.7038213e-08	1.703821
wall-12	0	0	0	0	0	0
walls	0	0.010705289	0.010705289	0	0.0010923765	0.001092
Net	0.052027349	0.014635897	0.066663247	0.0053089132	0.0014934589	0.006802

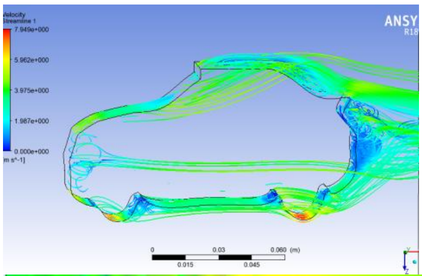

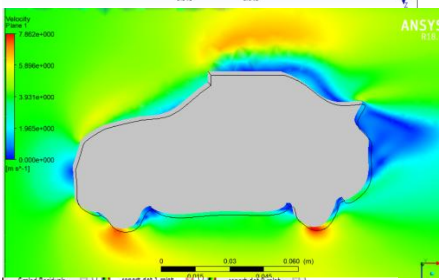

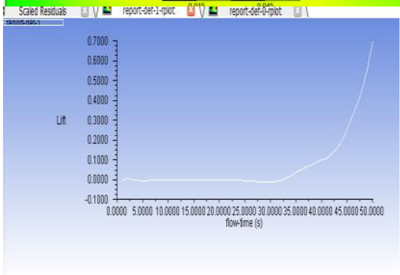

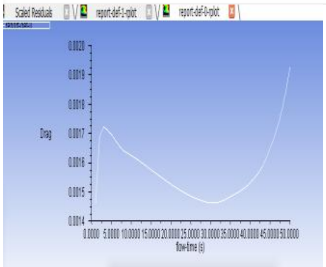

Forces - Direction Vector (1 0 0)

	Forces (n)			Coefficients		
Zone	Pressure	Viscous	Total	Pressure	Viscous	Total
wall-6-shadow	35.381267	0.28780332	35.66907	3.6103334	0.029367685	3.639701
wall-6	0	0	0	0	0	0
wall-13	1.321528e-06	1.0847787e-06	2.4063067e-06	1.348498e-07	1.1069171e-07	2.455415
wall-12	0	0	0	0	0	0
walls	0	-0.018861182	-0.018861182	0	-0.0019246104	-0.00192
Net	35.381268	0.26894322	35.650211	3.6103335	0.027443186	3.63776

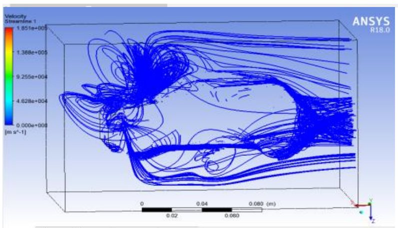

ISSN: 2456-219X
Journal Of Mechanical Engineering And Biomechanics   Volume 11 Issue 1 April 2026

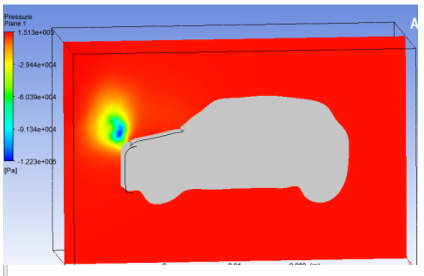

Forces - Direction Vector (1 0 0)

	Forces (n)			Coefficients		
Zone	Pressure	Viscous	Total	Pressure	Viscous	Total
wall-6-shadow	3.6755479	7.4937662	11.169314	0.37505591	0.76467002	1.13972
wall-6	0	0	0	0	0	0
wall-13	-4.0973453e-09	-1.537507e-06	-1.5416044e-06	-4.1809646e-10	-1.5688847e-07	-1.5730
wall-12	0	0	0	0	0	0
walls	0	-0.013221734	-0.013221734	0	-0.0013491565	-0.0013
Net	3.6755479	7.480543	11.156091	0.37505591	0.76332071	1.13837

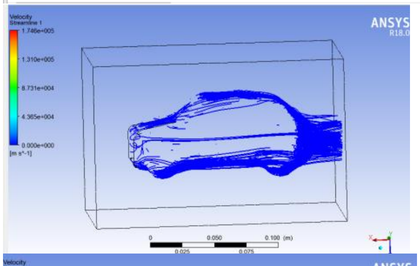

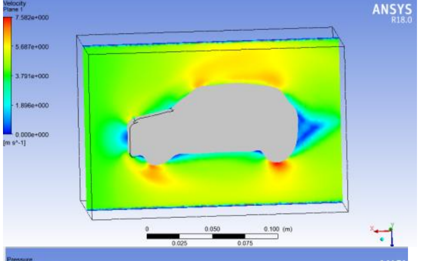

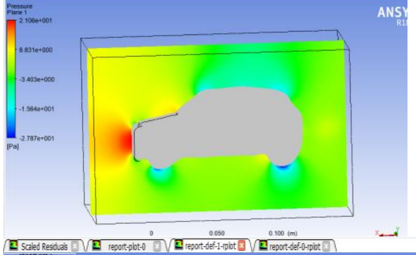

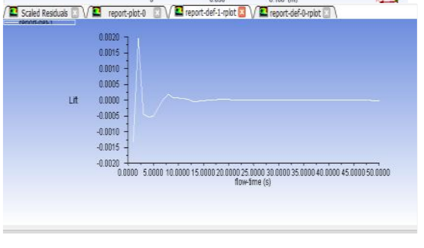

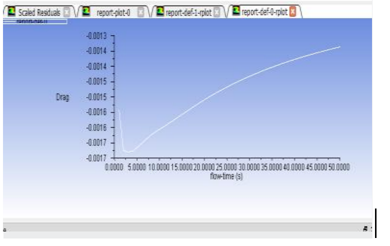

Forces - Direction Vector (1 0 0)

	Forces (n)			Coefficients		
Zone	Pressure	Viscous	Total	Pressure	Viscous	Total
wall-6-shadow	0.020166157	0.0032360985	0.023402255	0.0020577711	0.00033021413	0.002387[illegible]
wall-6	0	0	0	0	0	0
wall-13	4.365652e-20	1.308901e-07	1.308901e-07	4.454747e-21	1.3356133e-08	1.335613[illegible]
wall-12	0	0	0	0	0	0
walls	0	0.013101297	0.013101297	0	0.001336867	0.001336[illegible]
Net	0.020166157	0.016337526	0.036503683	0.0020577711	0.0016670945	0.003724[illegible]

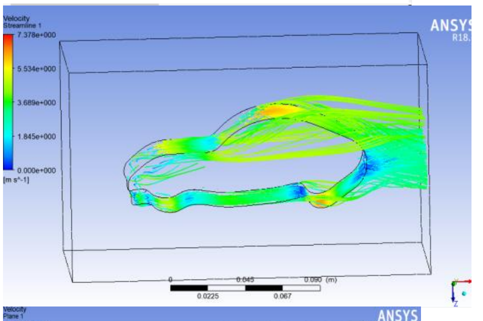

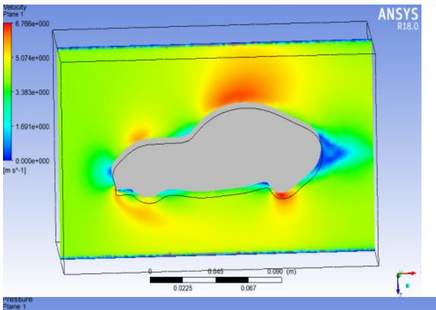

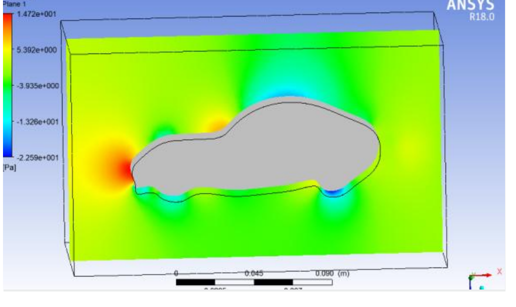

ISSN: 2456-219X
Journal Of Mechanical Engineering And Biomechanics Volume 11 Issue 1 April 2026

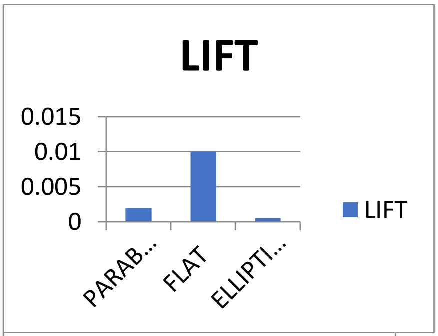

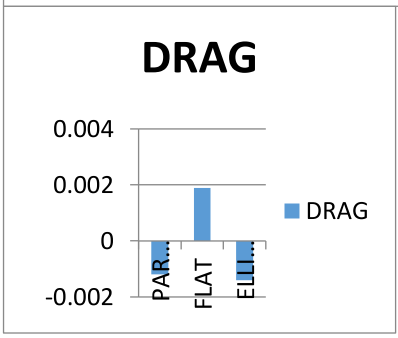

This study presents a CFD-based investigation of aerodynamic drag and lift acting on a road vehicle. The results confirm that pressure drag, originating from flow separation at the rear end, is the dominant component of total drag. Streamlined rear-end geometries such as elliptical and notchback designs significantly reduce wake size and improve pressure recovery, resulting in lower drag coefficients.

The analysis also highlights the influence of wheel rotation, engine cooling airflow, and underbody flow on aerodynamic performance. CFD proves to be an effective and economical tool for evaluating vehicle aerodynamics and guiding design optimization. Future work may include transient simulations and detailed optimization studies under realistic crosswind conditions.

References

6.Comparison with Experimental Trends

The numerical results show good qualitative agreement with experimental findings reported in literature for generic vehicle shapes. Trends in drag variation with rear slant angle and wake behaviour are consistent with wind tunnel observations, validating the adopted CFD methodology.

7. Conclusion

Wolf-Heinrich Hucho, Aerodynamics of Road Vehicles, 4th Revised Edition, Society of Automotive Engineers, U.S., 1998, ISBN: 978-0768000290

ChanchanRajsinhB. And ThundilKarippa Raj R; Numerical Investigation of External Flow around the Ahmed Reference Body using computational Fluid Dynamic; Research Journal of Recent Science; Vol.1(9),1-5, September 2012.

Ambeprasad.S.Kushwaha; Comaparative Study of Rectangular, Trapezoidal and Parabolic Shaped Finned Heat sink; e- ISSN: 2278-1684 Volume 5; Issue 6;(Mar. – Apr. 2013)

Vittorio Celli; Univ. of Verginia; Boundary layer separation and pressure drag; EDT 1997; http://galileo.phys.virginia.edu/classes/311/notes/fluids2/node11.html

Wake;Wikipedia;14 April 2016;https://en.wikipedia.org/wiki/Wake

Frank Werner, Steffen Frik, Adam Opel AG, Josepf Schulze; Aerodynamics Optimization of the Opel Calibra ITC Racing car using experiments and computational fluid dynamics.homepage.ntlworld.com/hoglabs/docs/calibre_aerodynamics/aerodynamics.htm

K.V.S Pavan (May 2012- July2012); CFD Modelling of flow around Ahmed Body. es/www.cd_adapco.com/sitdefault/files/technical_document/pdf/PavanIITHyderbad.pdf

Oxford Brookes University school of technology (September 2012);Aerodynamic analysis and optimization of the rear wing of WRC car.www.cd_adapco.com/sites/default/files/technical_document/pdf/zpch%2011%200148_0.pdf

C. Hinterberger, M. Garica-Villalba and W. Rodi; large eddy simulation of flow around the Ahmed body. user.engineering.uiowa.edu/˜me_160/lab/LESahmedcurrod.pdf.